Paper No. 1226. (quote when citing this article)
Eleventh World Conference on Earthquake Engineering
ISBN: 0 08 042822 3

INELASTIC BEHAVIOR OF STEEL FRAMES WITH STEEL BEAM SEISMIC ENERGY DISSIPATION DEVICE

MITSUMASA MIDORIKAWA[1], ISAO NISHIYAMA[2], and MITSURU SUGISAWA[3]

1)Head of Structure Division, Building Research Institute, Ministry of Construction,
1 Tatehara, Tsukuba, Ibaraki, 305 Japan
2)Coordinator for International Research Cooperation, Building Research Institute, Ministry of Construction,
1 Tatehara, Tsukuba, Ibaraki, 305 Japan
3)Senior Manager, Building Research Development, Nippon Steel Corporation,
20-1 Shintomi, Futtsu, Chiba, 299-12 Japan

ABSTRACT

The building response to a severe earthquake motion can be reduced or controlled by increasing the dissipation energy caused by plastic deformations of energy dissipation members/devices built into a frame structure. The inelastic behavior of three steel frames with steel beam energy dissipation (SBED) device was investigated through a series of cyclic loading tests to evaluate their seismic performance and possible use of structural seismic energy dissipation systems. Three single-bay, single-story steel frames with SBED device were designed and fabricated. The SBED device was located between the girder and the inverted-V brace. The girders, columns, and braces of the test frames had wide flange sections of mild steel. Each of test frames had different types of SBED device, that is, wide flange beams of hybrid sections made of different grades of steel between the flange and web: i) mild steel for flange and low-yield-point steel for web; ii) mild steel for flange and super-low-yield-point steel for web, and ; iii) high-strength steel for flange, super-low-yield-point steel for upper-half web, and mild steel for lower-half web. Each test frame was subjected to cyclic horizontal load. Evaluated was mainly the inelastic behavior of the test frames: the inelastic deformation capacity, the initial yield story shear corresponding to shear yielding of the SBED device, the yield and maximum story shears, and the energy dissipation capacity. The test results show that the steel frames with SBED device have many desirable attributes as seismic energy dissipation system, and that the SBED devices efficiently dissipate the energy compared with the frame members.

KEYWORDS

inelastic behavior; steel frame; cyclic loading test; seismic energy dissipation device; hybrid section; low-yield point steel; hysteretic behavior; failure mode; shear strength; energy dissipation capacity.

INTRODUCTION

The horizontal response of a structure exceeded the acceleration of 1 g during major earthquakes represented by the 1994 Northridge and the 1995 Hyogoken-nanbu (Kobe) Earthquakes. The current seismic design of building structures is based on this level of response. The general idea is that a building can survive a severe earthquake without collapse with a significant amount of inelastic behavior. According to the energy concept (Akiyama, 1985) introduced to the seismic design of buildings, the adequate seismic performance of a building structure can be accomplished if the energy capacity to be absorbed by the structure, while the structure responds to a severe ground motion, exceeds the total input energy exerted by the ground motion. On the other hand, the recent earthquake damages to buildings have raised an important question about the current seismic design philosophy which anticipates the inelastic deformation capacity of frame members themselves, such as beams and columns, against major earthquakes. Consequently, the advanced structural system incorporating seismic energy dissipation members/devices into a building structure (Steering Comm. of Symp., 1995) has been pursued. The building response to a severe earthquake motion can be reduced or

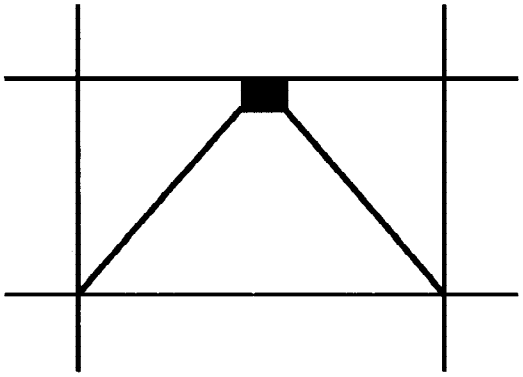

Fig. 1 Energy dissipation device built into frame

controlled by increasing the dissipation energy caused by plastic deformations of energy dissipation devices built into a frame structure as shown in Fig. 1.

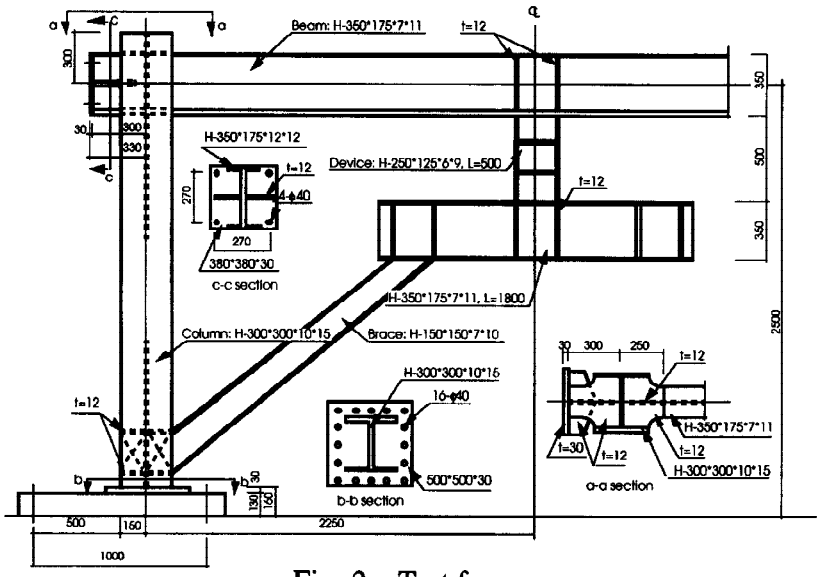

Fig. 2 Test frame

Many applications in the field of energy dissipation devices can be found in the literature (Seki *et al.*, 1988; SMiRT11, 1991; Izumi *et al.*, 1992; Steering Comm. of Symp., 1995; Saeki *et al.*, 1995; Nakashima, 1995). Steel plate energy dissipation devices were tested on the shaking table by Whittaker *et al.* (1991). Some of pioneer studies on eccentric structural steel bracing systems were reported by Fujimoto *et al.* (1972), and Roeder and Popov (1978).

In this paper, an investigation of the inelastic behavior of three steel frames with steel beam energy dissipation (SBED) device, through a series of cyclic loading tests, is presented. The mechanical performance is assessed in context of possible use of the test frames as seismic energy dissipation system. The SBED device was located between the girder and the inverted-V brace of single-bay, single-story test frames. Each of test frames had different types of SBED device, that is, wide flange beams of hybrid sections made of different grades of steel between the flange and web. The hybrid sections are quite effective in increasing the energy dissipation capacity of the devices under cyclic loading, compared with the non-hybrid sections, as shown in the previously reported results (Takeuchi *et al.*, 1992; Nishiyama and Midorikawa, 1992, 1993; Midorikawa *et al.*, 1994a, 1994b; Nagatsuka *et al.*, 1994; Nishiyama *et al.*, 1995). The test frames were subjected to cyclic horizontal load. Of main interest were: the inelastic deformation capacity, the initial yield story shear corresponding to shear yielding of the SBED device, the yield and maximum story shears, and the energy dissipation capacity.

EXPERIMENTAL ARRANGEMENT

Test Frames and Energy Dissipation Devices

Three single-bay, single-story steel frames with SBED device, Frames A, B, and C, were designed as weak column-strong beam moment-resisting frame with the inverted-V brace as shown in Fig. 2. The SBED device was located between the girder and the inverted-V brace. The braces were proportioned not to buckle at the ultimate strength of the test

Table 1 Dimensions of test frames

Frame	A	B	C
Story height (cm)	234		
Span (cm)	450		
Column	H-300x300x10x15		
Beam	H-350x175x7x11		
Brace	H-150x150x7x10		
Device	BH-250x125x6x9		
Flange	SS400	SS400	SM490A
Web	LYP235	LYP100	LYP100
			SS400

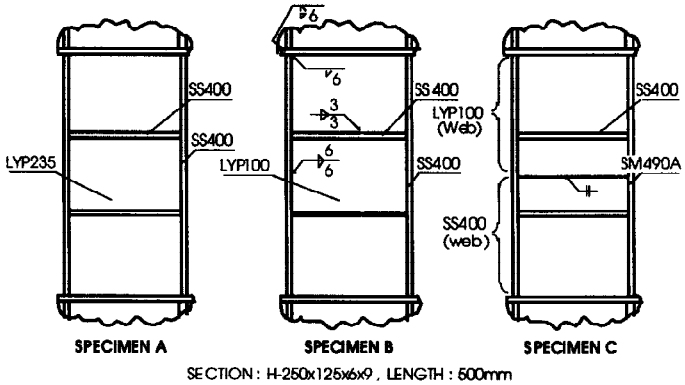

Fig. 3 Energy dissipation devices

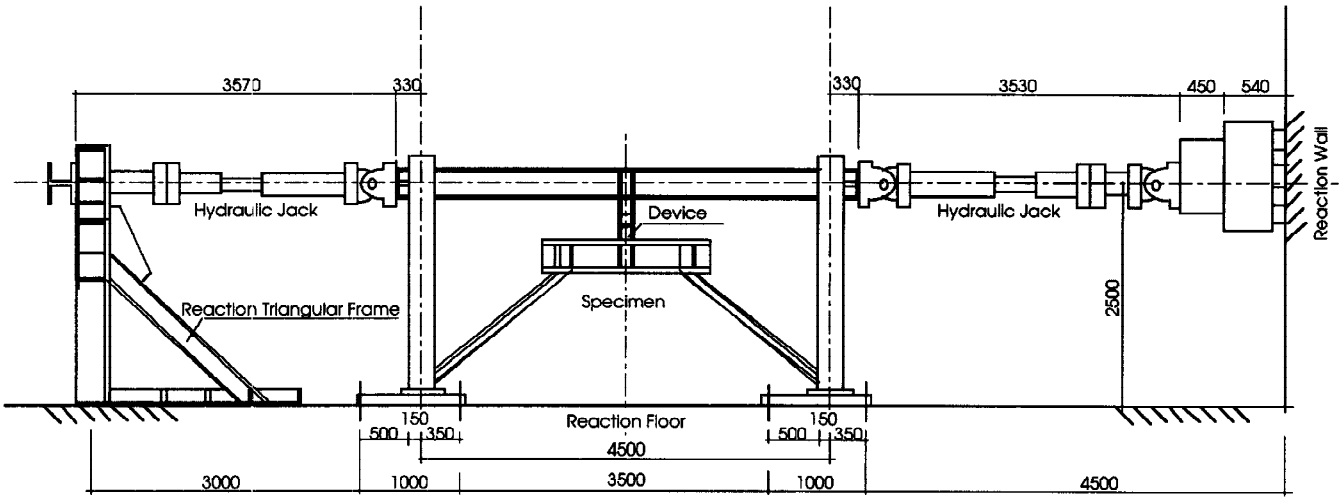

Fig. 4 Test setup

frames. The columns were arranged to be subject to bending about the minor axis. The test frames were fabricated by welding. The girders, columns, and braces of the test frames had rolled wide flange sections of mild steel (SS400). Table 1 shows the dimensions of the test frames. Each of test frames had different types of SBED device as shown in Fig. 3, that is, built-up wide flange beams of hybrid sections made of different grades of steel between the flange and web: i) mild steel for flange and low-yield-point steel (LYP235) for web in Frame A; ii) mild steel for flange and super-low-yield-point steel (LYP100) for web in Frame B, and ; iii) high-strength steel (SM490A) for flange, super-low-yield-point steel for upper-half web, and mild steel for lower-half web in Frame C. The SBED devices were 500 mm in length with aspect ratio of two. The flanges of the SBED device were connected at both ends with partial penetration welds, while other connections were made with fillet welds. Double-sided intermediate stiffeners (to prevent the web buckling) and link beam stiffeners (to preclude the possibility of flange buckling) were provided with spacing determined according to the eccentrically braced frame requirements of UBC (1991). Table 2 summarizes the flange and web plate mechanical properties for each steel obtained from the coupon tests.

Table 2 Mechanical properties of steel

Metal	Tensile strength σ_u (tonf/cm^2)	Yield strength σ_y (tonf/cm^2)	Uniform strain (%)	Elongation (%)
LYP100 t=6mm	2.309	0.867	33	46
LYP235 t=6mm	3.391	2.422	28	35
SS400 t=9mm	4.457	2.960	21	29
SS400 t=6mm	4.755	3.315	22	28
SM490A t=9mm	5.433	3.946	18	23
H-300x300x10x15	flange: 4.409	flange: 2.752	flange: 22	flange: 32
	web: 4.538	web: 3.117	web: 22	web: 29
H-350x175x7x11	flange: 4.573	flange: 3.272	flange: 23	flange: 30
	web: 4.829	web: 3.828	web: 18	web: 21
H-150x150x7x10	flange: 4.480	flange: 3.145	flange: 23	flange: 30
	web: 4.676	web: 3.487	web: 20	web: 24

Test Setup and Loading Program

Figure 4 shows the test setup fixed to the reaction floor through the reaction plates. The frames were tested by quasi-statically cyclic loading. The horizontal loads were applied equally to each top of columns. In the loading tests, the completely reversed story displacement was gradually increased by a certain story drift angle, expressed as a multiple of 0.005 radian. The story drift angle is defined as the story displacement divided by the story height.

RESULTS AND DISCUSSION

Test Results

The test results are summarized in Table 3. They include: the elastic stiffness, Ke, the yield story shear strength, Qy, the maximum story shear strength, Qmax, the stable story drift amplitude, Damp, the critical dissipation energy, Wmax, and the failure mode for each test frame. The stable story drift amplitude, Damp, is determined as the maximum story drift angle of the hysteresis loop which shows no definite degradation in

Table 3 Summary of test results

Frame	Elastic stiffness Ke (tonf/cm)	Yield story shear strength Qy (tonf)	Maximum story shear strength Qmax (tonf)	Stable story drift amp. Damp (radian)	Critical dissipation energy Wmax (tonf·cm)	Failure mode
A	83.7	23.5	83.4 (46.8, 36.6)[a]	0.042	9503	Device shear yield,
			-82.7 (-46.7, -36.0)	-0.043	(3979, 5524)[b]	frame flexural yield,
	89.4 [c]	*26.6*	*64.7 (37.6, 27.1)*			and device web fracture
B	81.4	6.4	73.1 (46.9, 26.2)	0.061	10721	Device shear yield,
			-73.6 (-47.4, -26.2)	-0.049	(5608, 5113)	frame flexural yield, and
	89.4	*8.8*	*54.7 (37.6, 17.1)*			beam lateral buckling
C	101.7	6.0	76.8 (49.0, 27.8)	0.038	5393	Device shear yield,
			-76.4 (-44.7, -31.7)	-0.032	(2429, 2964)	frame flexural yield,
	89.4	*8.8*	*54.7 (37.6, 17.1)*			and device web fracture

Notes: a) Numerals in the parentheses show the shear force carried by the frame and the device portions, respectively.
b) Numerals in the parentheses show the critical energy dissipated by the frame and the device portions, respectively.
c) Numerals in *italics* are the calculated results.

strength or stiffness. Wmax is the energy dissipated up to the critical point of the hysteresis loop, where the story shear force reduces to 95% of the peak shear force in a half-loading cycle. The calculated results using the coupon test results are shown in italics in Table 3. The calculated yield story shear strength, Qy, corresponds to the story shear strength of the test frame when the SBED device reaches the yield shear strength. The maximum story shear strength of the test frame is determined by the ultimate column flexural strength and the ultimate device shear strength. Therefore, the calculated maximum story shear strength, Qmax, corresponds to the sum of the ultimate column flexural strength reaching the full plastic moment and the ultimate device shear strength reaching the ultimate shear using $\sigma_u/\sqrt{3}$ for the whole web section. Figure 5 shows the story shear versus story drift relationships of the test frames, while Fig. 6 shows the shear versus drift angle relationships of the devices. The device shear is obtained by subtracting the column shears from the story shear.

Hysteretic Behavior and Failure Modes

Figures 5(a) through (c) show the story shear versus story drift relationships of the test frames. Each test frame can withstand the large inelastic deformations without definite deterioration of hysteresis loops or degradation in strength or stiffness up to the story drift amplitude of -0.043 to 0.042, -0.049 to 0.061, and -0.032 to 0.038 radians for Frames A, B, and C,

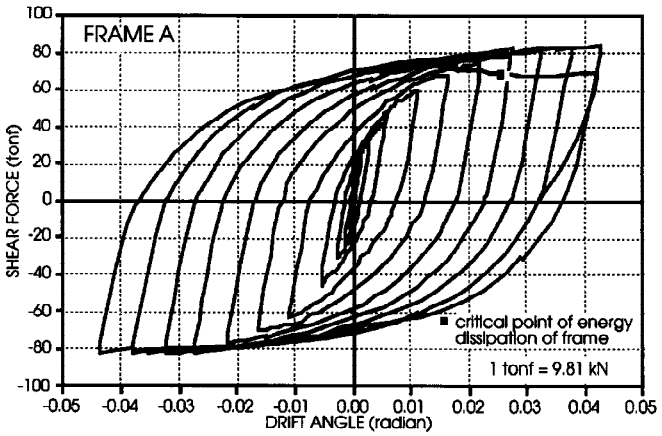

Fig. 5(a) Story shear vs. story drift relationship: Frame A

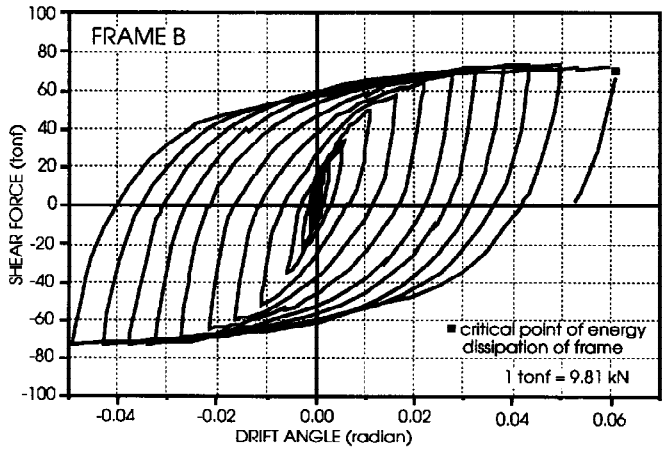

Fig. 5(b) Story shear vs. story drift relationship: Frame B

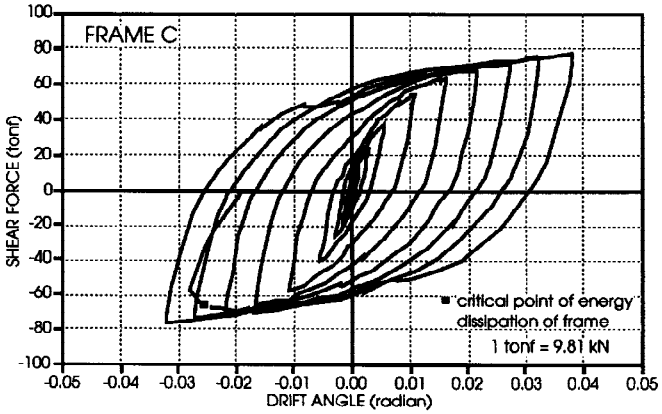

Fig. 5(c) Story shear vs. story drift relationship: Frame C

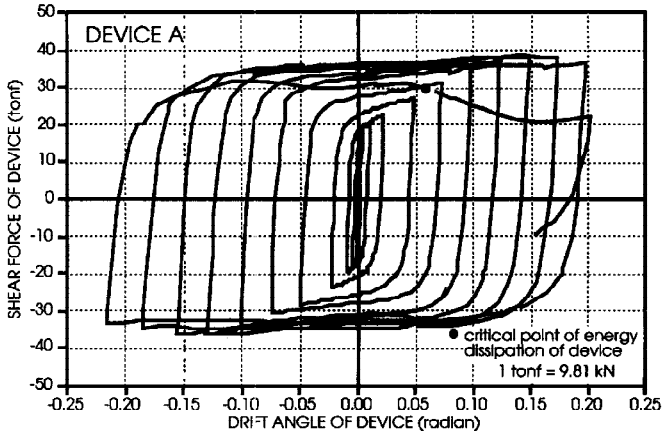

Fig. 6(a) Shear vs. drift angle relationship of device (LYP235): Frame A

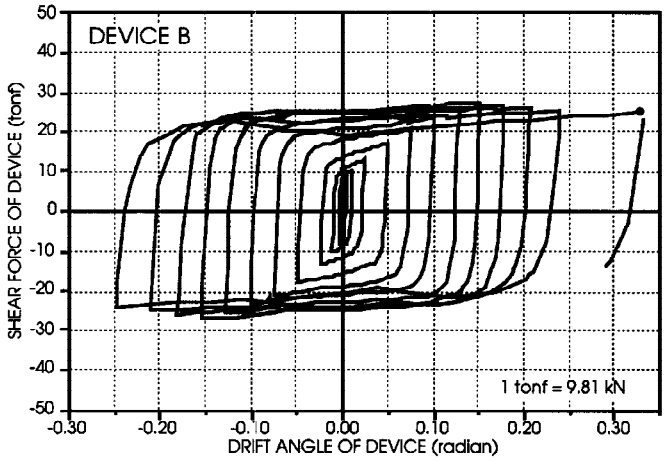

Fig. 6(b) Shear vs. drift angle relationship of device (LYP100): Frame B

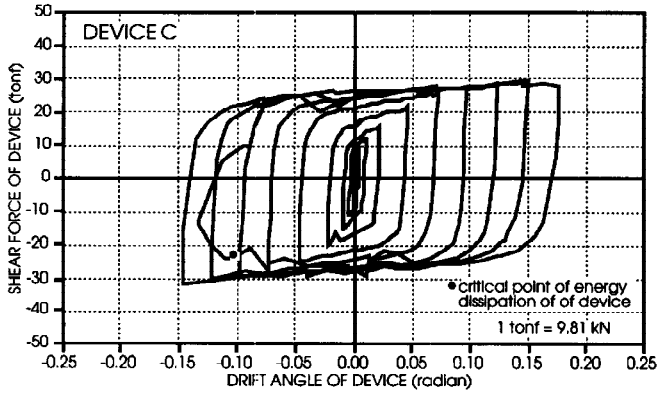

Fig. 6(c) Shear vs. drift angle relationship of device (LYP100 & SS400): Frame C

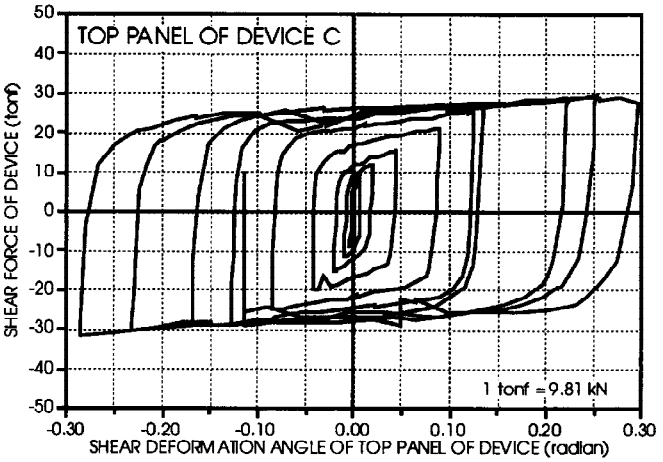

Fig. 7(a) Shear vs. shear deformation angle relationship of top panel of device in Frame C

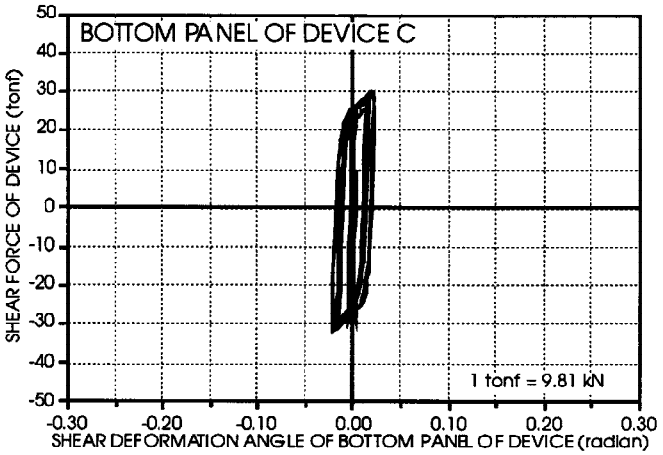

Fig. 7(b) Shear vs. shear deformation angle relationship of bottom panel of device in Frame C

respectively. Frame A shows the reduction in strength when going toward the story drift amplitude over 0.042 radian, due to the fracture of stiffener-to-web fillet welds at heat affected zone of the SBED device, following the shear yielding of the device, the local buckling of column flanges at both column ends, and the cyclic shear buckling of device web. In Frame B, the inelastic lateral buckling of the beam caused the very slight degradation in strength over the story drift amplitude of 0.05 radian, following the shear yielding of the device, the local buckling of column flanges at both column ends, the cyclic shear buckling of device web, and the fracture of web-to-flange fillet welds at heat affected zone of the device. In Frame C, the reduction in strength occurred when approaching the story drift amplitude of -0.038 radian, due to the fracture of stiffener-to-web fillet welds at heat affected zone of the device, following the shear yielding of the device, the shear buckling of device web, and the slight local buckling of column flanges at both column ends.

Figures 6(a) through (c) show the shear versus drift angle relationships of the devices. The devices have the stable hysteresis loops up to the drift angles of 0.20, 0.25, and 0.15 radians for Frames A, B, and C, respectively. The hysteresis loops show the slight reduction in strength near the neutral drift angle, which corresponds quite well with the jump of the web buckling mode due to the reversed loading effect. The ratio of the device drift to the story drift is roughly equal to 4.7 that is the ratio of the story height (234 cm) to the device length (50 cm), because the inverted-V brace is much stiffer than the device. Figure 7 shows the shear versus shear deformation angle relationships of the top and bottom panels of the device in Frame C. The maximum shear deformation of the top panel is about ten times as much as that of the bottom panel. It is

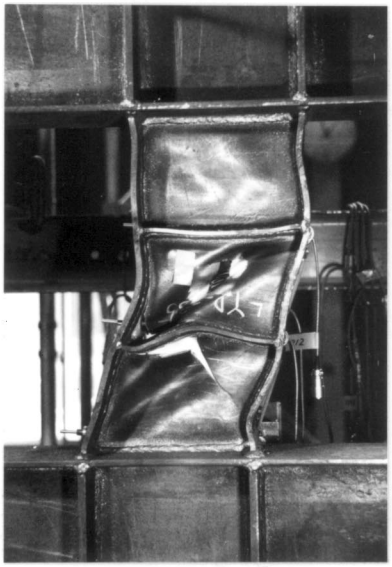

Fig. 8(a) Device in Frame A

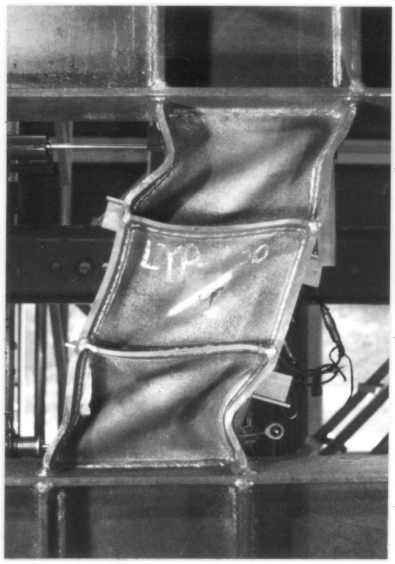

Fig. 8(b) Device in Frame B

Fig. 8(c) Frame C at the end of testing

clear that the shear deformation concentrates in the upper half of device web made of super-low-yield-point steel (LYP100). Figures 8(a) through (c) show the photographs of the failure modes of the devices in Frames A and B, and Frame C at the end of testing.

Yield and Maximum Shear Strength

Table 3 indicates that the ratio of the measured yield story shear strength, Qy, to the calculated strength is 0.88, 0.73, and 0.68 for Frames A, B, and C, respectively. The measured yield story shear strength is conservative because it corresponds to the initial shear yielding of the SBED device determined from the strain gauge measurement at the center of device web of the test frames. The general yielding of story shear is rather in good agreement with the calculated strength of 57, 44, and 44 tonf for Frames A, B, and C, respectively, which is the sum of the ultimate column flexural strength reaching the full plastic moment and the device yield shear strength reaching the shear yielding for the whole web section.

The maximum story shear strength, Qmax, of Frames A, B, and C is 28%, 34%, and 40% greater, respectively, than the calculated strength which corresponds to the sum of the ultimate column flexural strength reaching the full plastic moment and the ultimate device shear strength reaching the ultimate shear. At the point of the maximum story shear, the column shears of Frames A, B, and C is 1.24, 1.25, and 1.19 to 1.30 times, respectively, as much as the calculated shears, while the device shear is 1.33, 1.53, and 1.63 to 1.85 times, respectively, as much as the calculated shear. Consequently, the increase in the maximum story shear strength over the calculated strength results mainly from the remarkable increase in the device shear strength. The increase in strength of the devices is consistent with the previously reported beam test results (Midorikawa *et al.*, 1994a, 1994b). According to the beam test results, the maximum shear strength of SM570Q/LYP235-C-2-DS beam nearly conforming with the device in Frame A was 37% greater than the calculated strength. The maximum shear strength of SS400/LYP100-C-2-DS beam agreeing exactly with the device in Frame B was 62% greater than the calculated strength. It is mainly due to the work-hardening effect by the inelastic loading reversal. The maximum shear strength of the device in Frame C is 6 to 21% greater than that in Frame B. This results from that the device in Frame C behaved as very short beam because of the concentration of shear deformation in the upper half of the device. This is also in accordance with the previously reported beam test results (Nishiyama and Midorikawa, 1992) that the device is shorter, the increase in the ultimate strength compared with the calculated value becomes larger.

Energy Dissipation Capacity

Figures 8(a) through (c) show the dissipated energy versus cumulative displacement relationships of the test frames. The cumulative displacement is defined as the sum of the sequentially cyclic story displacement of the test frame. The dissipated energy of the entire frame is indicated with a thick line, and the dissipated energy of the SBED device with a fine line. The critical dissipation energy of the test frames, Wmax, is the energy dissipated up to the critical point of the hysteresis loop, where the story shear force reduces to 95% of the peak story shear force in a half-loading cycle. The critical point of the test frames is shown with a square mark in Figs. 5 and 9.

The moment resisting frame in Frames A, B, and C dissipates 42%, 52%, and 45% of the critical dissipation energy, Wmax, respectively, while the device dissipates 58%, 48%, and 55%, respectively. On the other hand, the moment resisting frame in Frames A, B, and C carries 56%, 64%, and 59 to 64% of the story shear at the maximum strength, respectively, while the device carries 44%, 36%, and 36 to 41%, respectively. It is noted that the dissipation energy ratio of the device to the frame members is larger than the ratio of the story shear carried by the device to the frame members. Consequently, the devices efficiently dissipate the energy compared with the frame members.

The critical dissipation energy of the device is defined as the energy dissipated up to the critical point of the hysteresis loop of the device, where the shear force in the device reduces to 95% of the peak shear force in a half-loading cycle. The critical point of the hysteresis loop of the devices is shown with a circle mark in Fig. 6. The critical dissipation energy of the device in Frames A and B is 5450 and 5110 tonf•cm, respectively, that is 1.9 and 2.1 times as much as that of SM570Q/LYP235-C-2-DS and SS400/LYP100-C-2-DS beams in the previously reported beam test results (Midorikawa *et al.*, 1994a, 1994b). It is due to the restraint effect of rotation at the both ends of device by the frame members and the inverted-V brace.

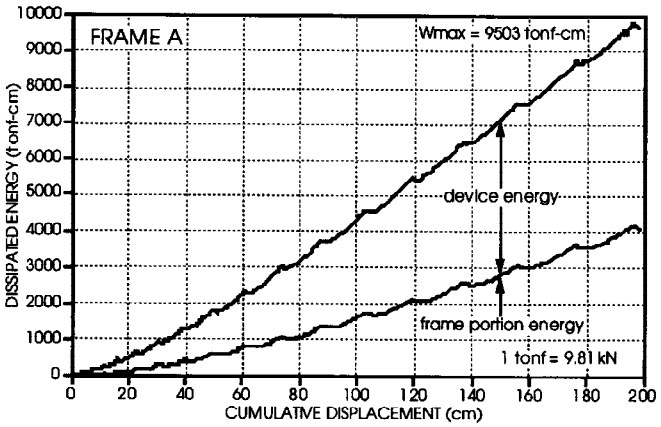

Fig. 9(b) Dissipated energy vs. cumulative displacement relationship: Frame B

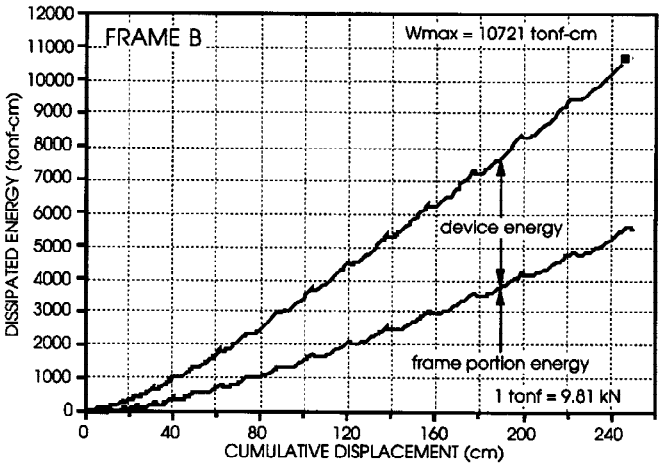

Fig. 9(b) Dissipated energy vs. cumulative displacement relationship: Frame B

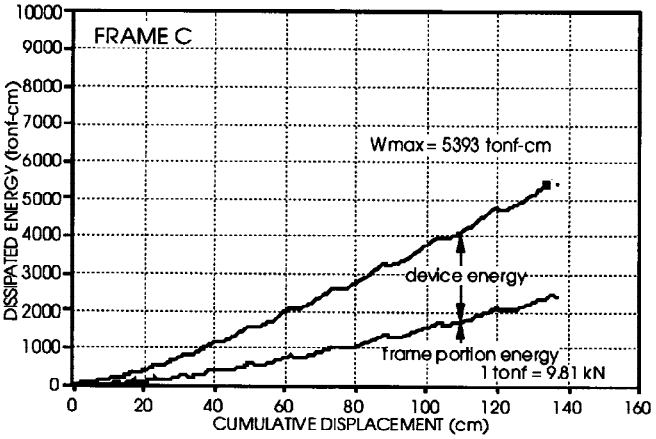

Fig. 9(c) Dissipated energy vs. cumulative displacement relationship: Frame C

CONCLUSIONS

The inelastic behavior of three single-bay, single-story steel frames with steel beam energy dissipation (SBED) device was investigated through a series of cyclic loading tests to evaluate their seismic performance and possible use of structural seismic energy dissipation systems. The SBED device was located between the girder and the inverted-V brace. Each of test frames had different types of SBED device that were wide flange beams of hybrid sections made of different grades of steel between the flange and web. The web of the devices was made of low-yield-point steel in Frame A, super-low-yield-point steel in Frame B, and super-low-yield-point steel for upper-half web and mild steel for lower-half web in Frame C. The test results show that the steel frames with SBED device have many desirable attributes as seismic energy dissipation system.

The conclusions drawn from the presented study can be summarized as follows;

(1) Each test frame shows the large deformation capacity and the stable hysteretic behavior under cyclic horizontal loading without definite deterioration or degradation in strength or stiffness up to the story drift amplitude of -0.043 to 0.042, -0.049 to 0.061, and -0.032 to 0.038 radians for Frames A, B, and C, respectively.

(2) The devices indicate the stable hysteresis loops up to the drift angle amplitudes of 0.20, 0.25, and 0.15 radians for Frames A, B, and C, respectively.

(3)The measured yield story shear strength, which corresponds to the initial shear yielding of the center of device web, is conservative compared with the calculated strength.

(4) The general yielding of story shear is rather in good agreement with the calculated strength of each test frame, which is the sum of the calculated ultimate flexural strength of columns and the calculated yield shear strength of device.
(5) The maximum story shear strength of Frames A, B, and C is 1.28, 1.34, and 1.40 times, respectively, as much as the calculated strength, which is the sum of the ultimate flexural strength of columns and the ultimate shear strength of device. It is mainly due to the work-hardening effect of the devices by the inelastic loading reversal.
(6) The dissipation energy ratio of the device to the frame members is larger than the ratio of the story shear carried by the device to the frame members. Consequently, the device in the test frames efficiently dissipates the energy compared with the frame members.

ACKNOWLEDGMENTS

This research was mainly sponsored by the Building Research Institute. The authors would like to express sincere gratitude to Nippon Steel Corp. for support and input provided during the course of the study. The authors also would like to express their appreciation to Dr. H. Fujitani and Mr. H. Endo for the assistance in testing and data processing.

REFERENCES

Akiyama, H. (1985). *Earthquake-Resistant Limit-State Design of Buildings*. University of Tokyo Press, Tokyo.

Fujimoto, M., T. Aoyagi, K. Ukai, A. Wada, and K. Saito (1972). Structural characteristics of eccentric K-braced frames. *Trans. of Arch. Inst. of Japan*, **195**, 39-49 (in Japanese).

Izumi, M., N. Kani, H. Narihara, K. Ogura, Y. Kawamata and O. Hosozawa (1992). Low cycle fatigue tests on shear yielding type low yield stress steel hysteretic damper for response control (part 1 and part 2). *Summaries of Tech. Papers of Annu. Meeting*, Structures **II**, AIJ, 1333-1336 (in Japanese).

Midorikawa, M., I. Nishiyama and M. Sugisawa (1994a). Cyclically inelastic behavior of seismic energy absorption steel members subjected to bending and shear. *1st World Conf. on Struct. Control*, **1**, Los Angeles, California, WP3-53-62.

Midorikawa, M., I. Nishiyama and M. Sugisawa (1994b). Inelastic behavior of short hybrid steel beams subjected to bending and shear. *Summaries of Tech. Papers of Annu. Meeting*, Structures **II**, AIJ, 1143-1144 (in Japanese).

Nagatsuka, N., I. Nishiyama, M. Midorikawa and M. Sugisawa (1994). Effect of energy dissipated metal member installed in steel frame. *Summaries of Tech. Papers of Annu. Meeting*, Structures **II**, AIJ, 1333-1334 (in Japanese).

Nakashima, M. (1995). Strain-hardening behavior of shear panels made of low-yield steel. I: Test. *J. Struct. Engineering*, ASCE, **121(12)**, 1742-1749.

Nishiyama, I. and M. Midorikawa (1992). Inelastic behavior of seismic energy absorption metal beams subjected to bending and shear. *Proc., Third Pacific Struct. Steel Conf.*, Tokyo, 481-488.

Nishiyama, I. and M. Midorikawa (1993). Inelastic behavior of short metal beams with aspect ratio 4 subjected to bending and shear. *Summaries of Tech. Papers of Annu. Meeting*, Structures **II**, AIJ, 1459-1460 (in Japanese).

Nishiyama, I., M. Midorikawa, M. Sugisawa, H. Fujitani and H. Endo (1995). Horizontal loading tests on portal frames with short steel beams of hybrid sections. *Summaries of Tech. Papers of Annu. Meeting*, Structures **III**, AIJ, 309-310 (in Japanese).

Roeder, C. W. and E. P. Popov (1978). Eccentrically braced steel frames for earthquakes. *J. Struct. Div.*, ASCE, **104(3)**, 391-412.

Saeki, E., Y. Maeda, H. Nakamura, M. Midorikawa and A. Wada (1995). Experimental study on practical-scale unbonded braces. *J. Struct. Constr. Engrg.*, AIJ, **476**, 149-158 (in Japanese).

Seki, M., H. Katsumata, H. Uchida and T. Takeda (1988). Study on earthquake response of two-storied steel frame with Y-shaped braces. Proc., *9th World Conf. on Earthquake Engrg.*, **IV**, Tokyo-Kyoto, 65-70.

SMiRT11 (1991). *Seismic Isolation and Response Control for Nuclear and Non-Nuclear Structures*. Special Issue for the Exhibition of the 11th Int. Conf. on Struct. Mech. in Reactor Tech., Tokyo.

Steering Comm. of Symp. (1995). *Proc., Symp. on a New Direction in Seismic Design*, Tokyo, Japan.

Takeuchi, T., I. Nishiyama and M. Midorikawa (1992). Inelastic behavior of short metal beams subjected to bending and shear. *Summaries of Tech. Papers of Annu. Meeting*, Structures **II**, AIJ, 1179-1180 (in Japanese).

UBC (1991). *Uniform Building Code, 1991 Edition*. Int. Conf. of Building Officials, Whittier, California.

Whittaker, A. S., V. V. Bertero, C. L. Thompson and L. J. Alonso (1991). Seismic testing of steel plate energy dissipation devices. *Earthquake Spectra*, **7(4)**, 563-604.